



Co-electrodeposition and properties evaluation of functionally gradient nickel coated ZrO₂ composite coating

B. BOSTANI¹, N. PARVINI AHMADI¹, S. YAZDANI¹, R. ARGHAVANIAN²

1. Faculty of Materials Engineering, Sahand University of Technology, Tabriz 53317-11111, Iran;

2. Department of Mechanical Engineering, Tabriz Branch, Islamic Azad University, Tabriz, Iran

Received 29 September 2016; accepted 22 March 2017

Abstract: For the first time, functionally electroless nickel plated ZrO₂ (NCZ) graded Ni-NCZ composite coating has been successfully co-electrodeposited from a bath with gradually increasing of stirring rate. Studies showed that co-electrodeposition in a bath with stirring rate of 250 r/min results in the maximum co-electrodeposited particle content and the best particle distribution. To produce NCZ graded Ni-NCZ composite coating, the stirring rate was continuously increased from 0 to 250 r/min. The electroplated coating had a continuous gradient increasing of co-electrodeposited NCZ content from substrate towards the surface. The results showed that with increasing the co-electrodeposited NCZ particles content in Ni matrix, microhardness increases from interface towards the surface of the coating. Little crystallite size of Ni matrix and higher co-electrodeposited hard particles content were recognized as the reasons of microhardness increasing. Bend test revealed that the functionally graded composite coating shows more excellent adhesion to the substrate compared with the ordinary distributed Ni-NCZ on the same substrate. This result is attributed to lower mechanical mismatch between coating and substrate in the functionally graded composite coating with respect to the uniformly distributed one. The results of wear resistance measurements reveal that wear resistance of functionally graded Ni-NCZ is higher than that of ordinary distributed composite coating.

Key words: co-electrodeposition; functionally graded composite coating; microhardness; wear resistance; adhesion

1 Introduction

Co-electrodeposition (CED) technique is a low-cost and low-temperature method suitable for producing metal matrix composite coatings for diverse purposes such as wear resistance, corrosion resistance, high-temperature corrosion protection, oxidation resistance, self-lubrication and abrasion resistance. These coatings typically contain oxide particles or carbide particles in micron, submicron and nano sizes, such as TiO₂, Al₂O₃, ZrO₂ and SiC, in an electrodeposited matrix [1–8]. To achieve desirable properties (such as high microhardness and corrosion resistance), it is necessary to increase the amount of uniformly distributed co-deposited particles in the coating. Higher amounts of co-deposited particles provide more nucleation sites for Ni clusters and more change in microstructure, which result in better properties [9–12].

Ceramic particles, being inert and hard, have been used more than the other particles in CED but these

particles lower the adhesion of the coating to the substrate, resulting in lower wear resistance and delamination and spallation of the coatings. On the other hand, co-deposited particles lower the grain size of the matrix so that mechanical mismatch between hard-brittle coating and soft-ductile substrate increases, leading to high stress concentration and weakness of the interface [13–18].

To avoid this deteriorating effect, functionally graded (FG) coatings are recommended [14,16]. It has been shown that functional grading of ceramic particles content in the deposits reduces delamination and spallation of the coatings [16]. The amount of ceramic particles can be gradually and functionally varied by changing the electrodeposition parameters, like current density, stirring rate, and particle content in the electrolyte [19–22].

In previous work, it has been shown that using NCZ particles as second phase in CED of Ni matrix composite coating enhances the microhardness and corrosion resistance [23], but to achieve desirable properties, it is

necessary to increase the amount of co-electrodeposited NCZ particles in the coating [24]. Ni coating on the surface of these particles (NCZ) could provide more nucleation sites for electrodepositing coating so that smaller grain sizes of electroplated Ni coating could be achieved. It seems that this little grain size could increase the mechanical mismatch between composite coating and the substrate. Our previous works [23] confirmed that the grain size of electroplate Ni coating is little for Ni-NCZ composite with respect to Ni-ZrO₂. This result shows the importance of mechanical mismatch between NCZ containing composite coatings and substrates. Although excellent corrosion resistance and microhardness have been obtained for Ni-NCZ composite, only a few works [23] have been done in the case of this composite coating probably due to the technical problems in synthesis of NCZ particles (electroless plating of ZrO₂ particles with Ni coating). Hence, for the first time in this work, functionally NCZ content graded Ni-NCZ composite coating by continuous variation of stirring rate is produced; and the adhesion and wear resistance between this gradient coating and the uniform composite coating is also compared.

2 Experimental

The ZrO₂ powder with a particle size of <5 μm was dispersed in an electroless Ni plating bath to be coated with a layer of electroless Ni coating. Pure Ni and Ni-NCZ composite coatings were electroplated from a Watt's bath. The compositions of the baths and the conditions of electroless and electroplating procedures are given in Table 1. To investigate the stirring rate effect on the co-electrodeposited second phase particles content in the coating, composite coatings were electroplated in a bath containing 90 g/L NCZ powder with various stirring rates. The stirring rate increased from 100 to 300 r/min with an increasing interval of 50 r/min. Also, NCZ content graded Ni-NCZ composite coating was electroplated in the same condition with continuous increasing of stirring rate. Coating surface morphologies were examined by employing scanning electron microscope (Cam Scan™ model MV2300 SEM operated

at 30 kV). Chemical composition of the coating was identified by using an energy dispersive X-ray spectroscopy (EDX) system (Oxford™) co-worked with the SEM. Five measurement trials were done and the results were averaged for each sample. Optical microscope was used to study particle distribution in the cross section of the samples. Microhardness assessment of the coating was performed using Vickers instrument (LECO™ AT-101) by applying 25 g load in 10 s. Four microhardness measurements were conducted and results were then averaged.

The XRD spectra of the samples were recorded, and (111) peak broadening of fcc nickel was used to determine the average crystallite size of the nickel matrix. Equation (1) (Scherrer equation) was used to calculate the crystallite size.

$$L = \frac{\lambda}{\beta \times \cos\theta} \quad (1)$$

where L is the crystallite size, λ is the X-ray wavelength, β is the effective line broadening and θ is the Bragg angle. β was obtained using the full width of the line measured at half maximum which was then corrected for instrumental broadening. For this correction, LaB₆ standard reference material (SRM 660a) was used.

The three-point bend test was carried out to compare the adhesion strength of the coatings on the st37 steel under a low strain rate at room temperature. The specimen sizes were 5 cm × 1.5 cm and the span between two supporting points was 3.5 cm.

Dry sliding wear tests were performed using a pin-on-disk wear apparatus at room temperature. The normal load of 6 N was used and the rotation speed was 50 r/min with a radius of 5 mm for 50 m sliding. Prior to wear test, all the contact surfaces were cleaned with acetone and dried. The wear loss and normalized wear rate were measured by an electric balance with 0.1 mg accuracy.

3 Results and discussion

3.1 Electrodeposition of ordinary Ni-NCZ (ON-NCZ) composite coating

In Fig. 1, the EDX mapping of NCZ powder shows

Table 1 Composition of baths and conditions of electro- and electroless-plating procedures

Condition	$\rho(\text{Nickel sulphate})/(\text{g}\cdot\text{L}^{-1})$	$\rho(\text{Nickel chloride})/(\text{g}\cdot\text{L}^{-1})$	$\rho(\text{Boric acid})/(\text{g}\cdot\text{L}^{-1})$	$\rho(\text{Sodium citrate})/(\text{g}\cdot\text{L}^{-1})$	$\rho(\text{Sodium dodecyl sulphate})/(\text{g}\cdot\text{L}^{-1})$	$\rho(\text{Sodium hypophosphite})/(\text{g}\cdot\text{L}^{-1})$	
Electroplating	250	40	45	50	0.1	–	
Electroless	35	–	–	15	0.2	20	
Condition	$\rho(\text{Sodium acetate})/(\text{g}\cdot\text{L}^{-1})$	Temperature/ °C	Plating time/h	Particle concentration/ $(\text{g}\cdot\text{L}^{-1})$	Current density/ $(\text{A}\cdot\text{dm}^{-2})$	pH	Stirring rate/ $(\text{r}\cdot\text{min}^{-1})$
Electroplating	–	54±1	1	90	3	3.8–4	0–300
Electroless	5	87±1	2	60	–	5.5–6	150

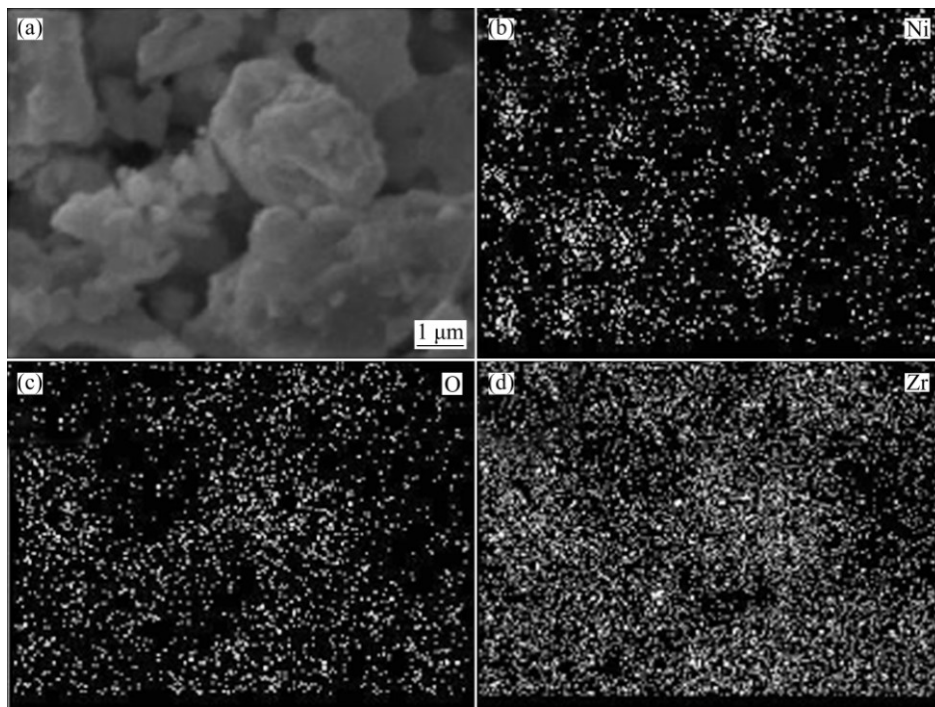


Fig. 1 SEM image (a) and corresponding EDX maps (b, c, d) of surface of NCZ particles

that electroless Ni coating is successfully deposited on the ZrO_2 particles surface.

The Zr content of the co-electrodeposited composite coatings as a function of stirring rate in the electroplating bath is shown in Fig. 2. It indicates that at a constant NCZ concentration in the bath, the co-electrodeposited NCZ particles content increases sharply with increasing stirring rate up to 250 r/min. As the stirring rate surpasses 250 r/min, the amount of co-electrodeposited NCZ particles decreases in the coating.

Figure 3 shows the surface morphology of the samples co-electrodeposited in the baths at stirring rates of 200, 250 and 300 r/min. It can be seen that stirring the bath at a rate of 250 r/min (Fig. 2(b)) results in maximum

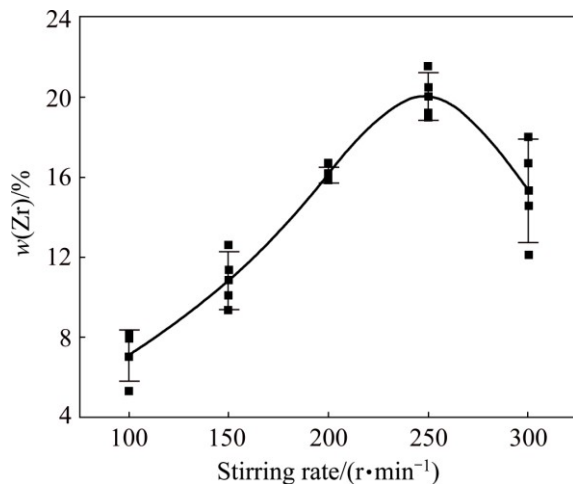


Fig. 2 Relationship between Zr content of composite coatings and stirring rate in electroplating baths

co-electrodeposition and the best distribution of NCZ particles in the coating. According to Guglielmi model [25], formation of composite coating in CED method has two steps. In the first step, the second-phase particles will be loosely adsorbed on the cathode surface by hydrodynamic and electrophoresis forces. In the second step, the ionic cloud will disappear and the particles will be strongly adsorbed on the cathode surface. It can be concluded that the stirring rate of the bath could have two opposite effects on the co-electrodeposited particles content. The first one is the positive effect which increases the content of incorporated particles. This effect is resulted from hydrodynamic flow. This flow can convey the particles in the bath to the surface of the electrodeposition layer and increase the incorporation of second phase particles in the coating. The second effect is the negative one which decreases the co-electrodeposited particles content in the coating. According to the Guglielmi model, in the first step, second-phase particles are loosely bonded to the cathode surface and a strong hydrodynamic flow could break these weak bonds and decrease the incorporation of the second phase particles in the coating. In the conditions of this work, below 250 r/min, the first effect (positive effect) predominates the second one (negative effect) and increasing of stirring rate results in more co-electrodeposition of second phase particles in the coating. Higher stirring rates cause strong hydrodynamic flows which make the particles to depart from the surface and the second effect (negative) becomes predominant so that the incorporation of particles decreases [26].

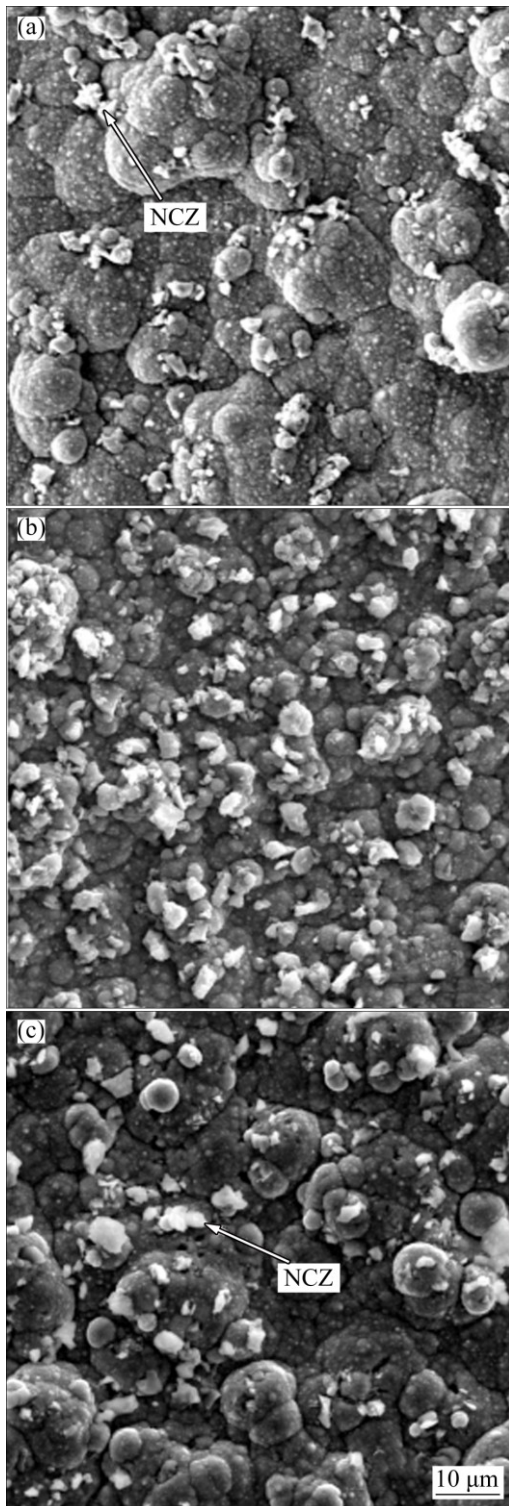


Fig. 3 SEM images of samples electroplated in baths at different stirring rates: (a) 200 r/min; (b) 250 r/min; (c) 300 r/min

Figure 4 shows the XRD patterns for the specimens electroplated in the baths at stirring rates of 200, 250 and 300 r/min. The relative intensity of NCZ diffraction peaks increases from the first to the second sample and then decreases, showing that the amount of NCZ in the

second sample (electroplated in the bath at stirring rate of 250 r/min) is higher than the other samples.

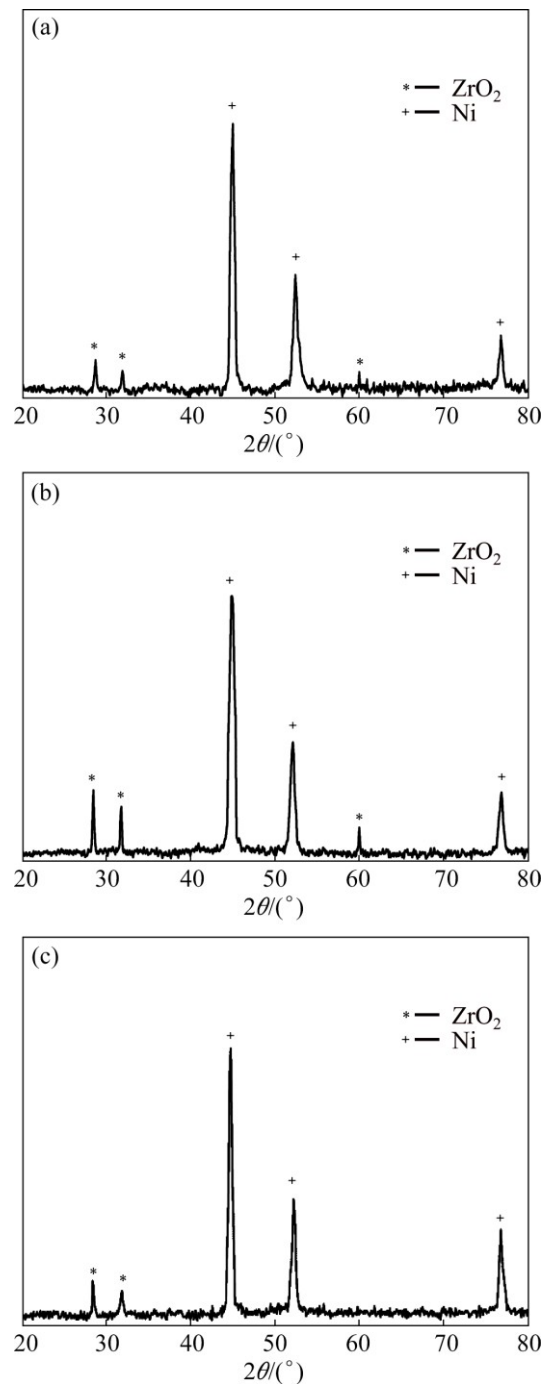


Fig. 4 XRD patterns of samples electroplated in baths at different stirring rates: (a) 200 r/min; (b) 250 r/min; (c) 300 r/min

Variations of Zr content, grain size of Ni and microhardness of composite coatings at various stirring rates are given in Table 2. The co-electrodeposited NCZ particles content increased by increasing stirring rate up to 250 r/min. This resulted in a finer grain size of Ni matrix and higher microhardness. Above 250 r/min, any increase in stirring rate indirectly led to decrease in

co-electrodeposited NCZ particles content, coarser Ni grains and lower microhardness.

Table 2 Zr content, crystallite size of Ni and microhardness values for Ni-NCZ composite coatings electroplated in baths at various stirring rates

Stirring rate/(r·m ⁻¹)	w(Zr)/%	Ni crystallite size/nm	Microhardness (VH ₂₅)
200	15.32±1	46	700
250	20.03±1	34	739
300	16.13±1	40	705

In previous work [10], it has been reported that the microhardness of Ni-ZrO₂ is about HV 600. Higher microhardness of Ni-NCZ could be due to the higher amount of co-electrodeposited second phase particles and smaller Ni matrix crystallite size. Another reason is the stronger bonds between Ni matrix and second phase particles in Ni-NCZ with respect to Ni-ZrO₂.

The wear track width and friction coefficients of the samples (resulted from wear tests) are given in Fig. 5. Figure 5(a) shows that the wear track width of pure Ni is larger than the composite coatings. Among these four coatings, the Ni-NCZ coating electroplated at 250 r/min has the lowest wear track width and the highest friction coefficient, which is matched by its highest microhardness.

3.2. Electrodeposition of functionally graded Ni-NCZ (FGN-NCZ) composite coating

The above-mentioned results revealed the experimental conditions which resulted in maximum microhardness in which the maximum co-electrodeposition of reinforcing particles (NCZ particles) in the coating remarkably reduces the grain size and this results in enhancement of microhardness. However, mechanical mismatch between the hard-brittle coating and the soft-ductile substrate has been recognized as the controlling factor for low adhesion and spallation of the coatings. To resolve this problem, FG composite coatings were also taken into account. In this way, the lower content of second phase particles close to the interface reduced mechanical mismatch and by approaching to the coating surface, the density of NCZ particles increased continuously. Technically, control of a parameter influencing on the co-electrodeposited particle content is of crucial importance in FG method. The results show that the stirring rate can be used to control the incorporated particles content in the coating. To produce FGN-NCZ composite coating, the stirring rate was continuously increased from 0 to 250 r/min, while the dispersed NCZ content in the Ni electroplating bath was 90 g/L.

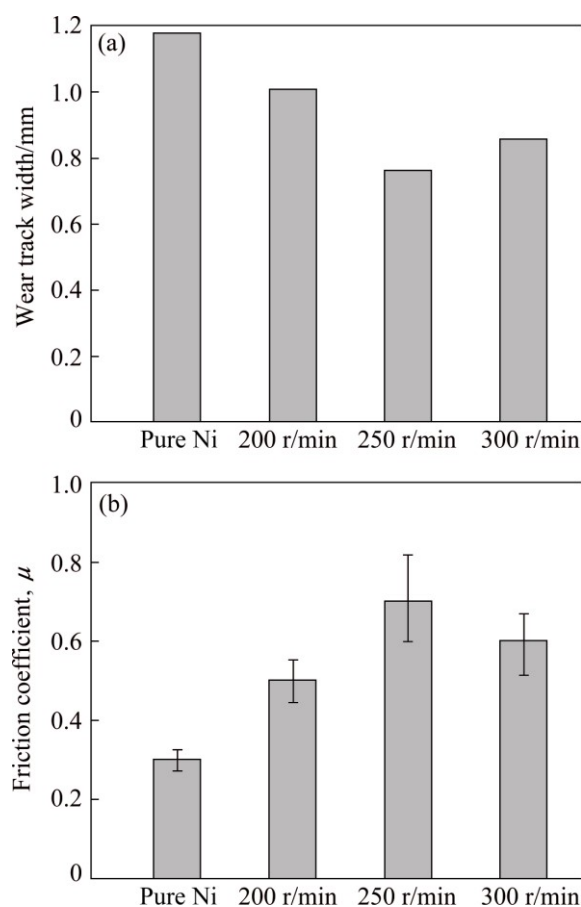


Fig. 5 Wear track width (a) and friction coefficient (b) of Ni-based coatings after wear tests

The EDX mapping of the cross-section of FGN-NCZ composite coating is demonstrated in Fig. 6, which indicates that the amount of second phase is increased from the interface to the surface. It could thus be stated that controlling stirring rate of the electroplating bath is a reliable route to successfully manufacture functionally graded composite coating.

Cross-sectional images of three electroplated samples in electrolytes at different stirring rates (200, 250 and 300 r/min) and FGN-NCZ composite coatings are illustrated in Fig. 7. This indicates that the highest co-electrodeposited NCZ particles content is achieved for the sample co-electrodeposited at stirring rate of 250 r/min (Fig. 7(b)). Also, it can be seen from Fig. 7(d) that in FGN-NCZ coating, NCZ particles are distributed with lower density in vicinity to the interface to higher density levels near the surface, forming a continuous gradient distribution of zirconia within the coating.

3.2.1 Microhardness

In Fig. 8(a), the variations of microhardness in the cross section of FGN-NCZ coating has been demonstrated. The size of indentation effects decreases from interface towards the surface of the coating.

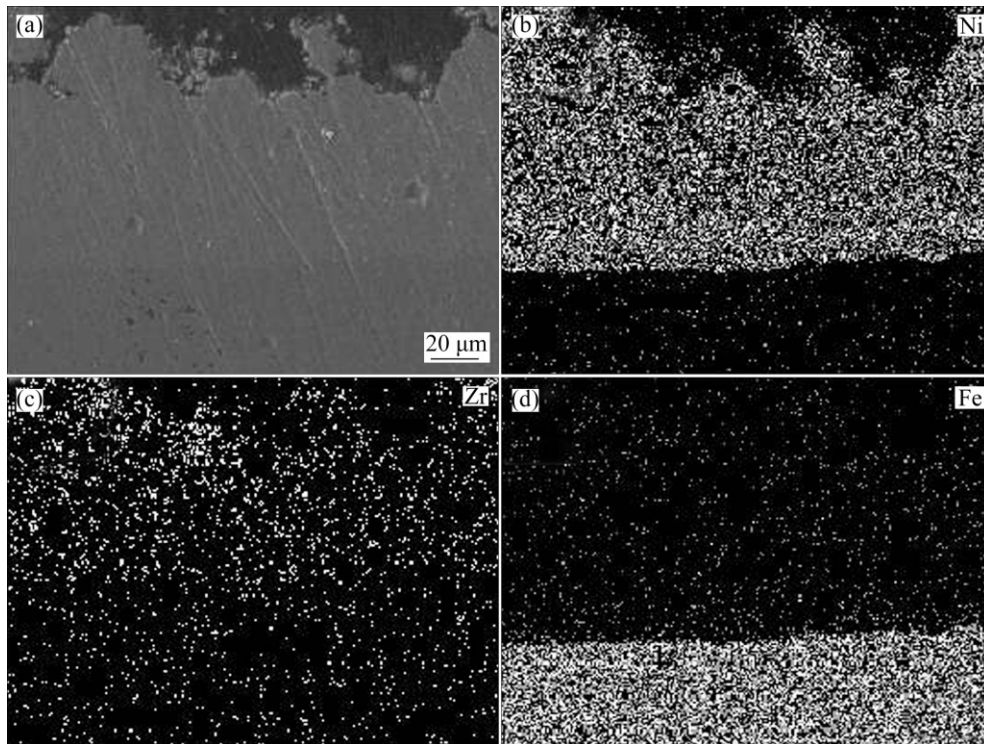


Fig. 6 SEM image (a) and corresponding distribution of nickel (b), zirconia (c) and iron (d) elements in FGN-NCZ coating

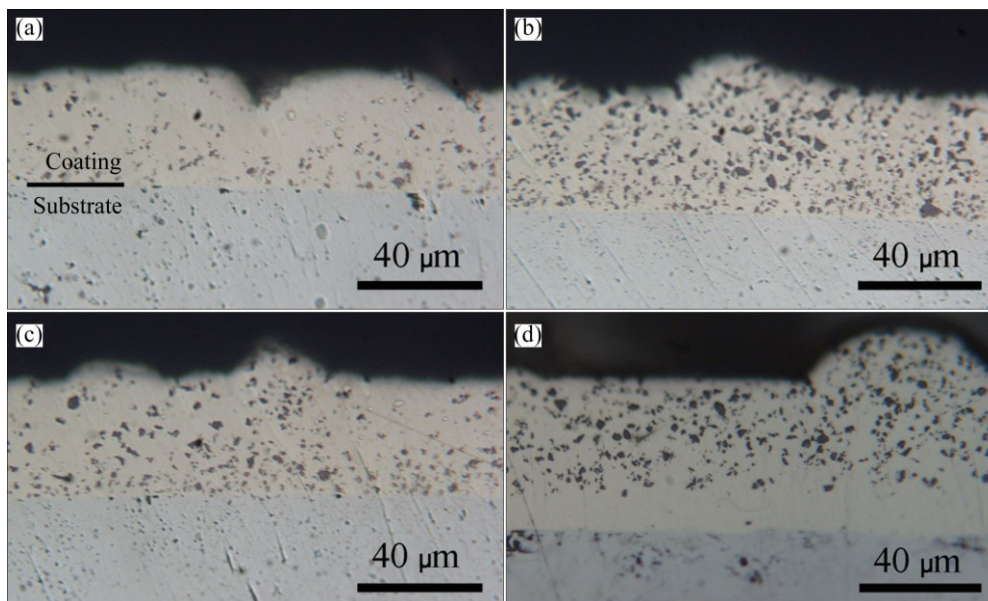


Fig. 7 OM cross-sectional images of composite coatings at different stirring rates: (a) 200 r/min; (b) 250 r/min; (c) 300 r/min; (d) FGN-NCZ

Figure 8(b) shows that microhardness increases gradually from HV 580 near the interface of the coating with the substrate to HV 730 near the surface of the coating. This is related to the simultaneous effect of the gradual increase in the amount of co-electrodeposited NCZ particles as well as the decrease in grain size of Ni matrix in FGN-NCZ coating from its interface with the substrate towards the surface. It should also be noted that

low microhardness of coating near the interface decreases the mechanical mismatch between the coating and its substrate. In this way, adhesion of the coating was enhanced and also risks of delamination and spallation decreased. Wear-resistant property of the coating also increased due to high microhardness near the surface.

3.2.2 Wear

Worn surfaces of the coatings are shown in Fig. 9.

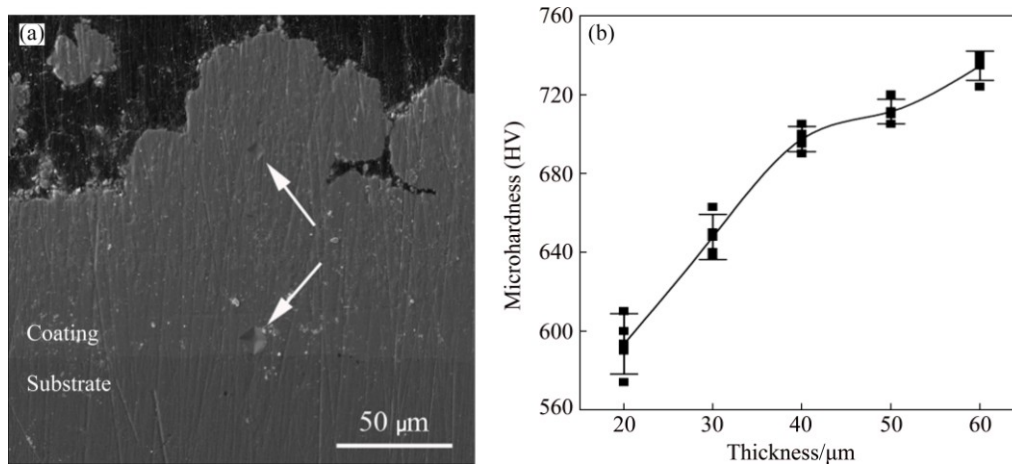


Fig. 8 Indentation effect of microhardness on cross-section of FGN-NCZ coating (a) and curve of microhardness versus thickness of FGN-NCZ coating (b)

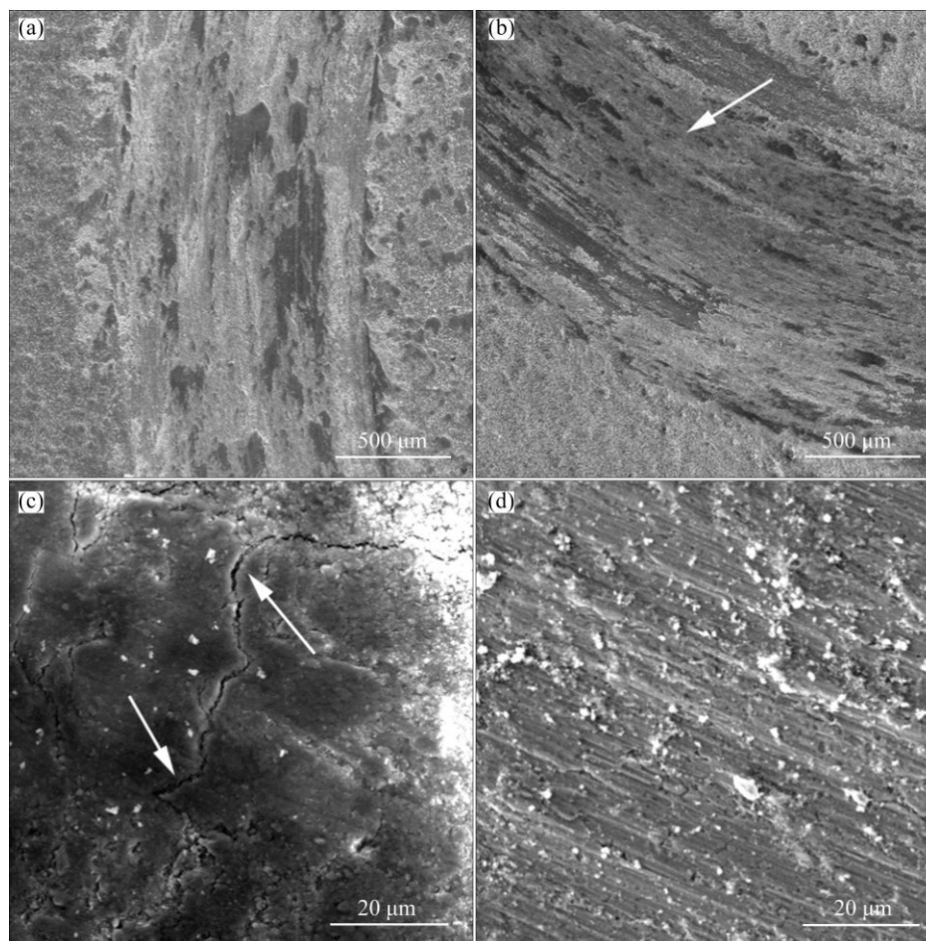


Fig. 9 SEM images showing worn surfaces of ON-NCZ (a, c) and FGN-NCZ (b, d) coatings at different magnifications: (a, b) Low magnification; (c, d) High magnification

Figures 9(a) and (c) show the wear track of the ON-NCZ composite coating worn surfaces. With addition of NCZ particles, the wear changed its mechanism nature from adhesive to abrasive because of the underlying properties of the NCZ particles. These particles could be separated from the matrix during wear applications which resulted in three body motions. The wear in this composite was

also abrasive because of the lack of plastic region for the coating but some cracks were observed as marked by arrows in Fig. 9(c). These cracks formed under high stress levels during the wear test. The micro-cracks might be typically the lateral fatigue cracks induced by tensile and compression stresses on the coating surface in sliding motions [27]. The propagation of these cracks

into the coating could be a reason for an earlier material removal [24]. Furthermore, the crack initiation caused considerable increase in mass loss of the ON-NCZ coating in comparison with that of the FGN-NCZ (Fig. 9). As shown in Figs. 9(b) and (d), the worn surface of FGN-NCZ coating has covered with a dark tribological layer excluding cracks. This tribological oxide layer has acted as a lubricant layer to reduce friction coefficient between the contact surfaces and confine the coating wear rate [28]. In the case of hard and brittle coatings on substrates, significant stress concentration occurred at the coating–substrate interface which might be responsible for initiation of macro-cracks and possible delamination of the ON-NCZ coating. However, it seemed that the particle gradient and the grain size in the FGN-NCZ coating towards the substrate considerably enhance the compatibility between coating and substrate, in contrast to those of the ON-NCZ coating. This significantly decreased the stress concentration at the coating– substrate interface leading to higher resistance to cracking and delamination. Moreover, it was believed that the gradient grain size microstructure of the FGN-NCZ coating enhances the resistance to the growth of the tribological cracks from the surface into the coating. Previous works stated that such microstructure presents higher resistance against crack initiation and growth than the uniform coatings [29].

The mass loss of the samples is shown in Fig. 10. Weighting of the coated samples and the steel pin before and after the wear test indicated that the minimum mass

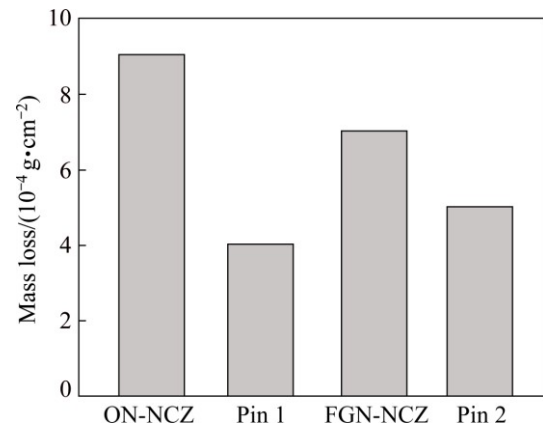


Fig. 10 Mass loss of coatings and corresponding material removal rate of pins

loss of the coating and maximum mass loss of the related pin are achieved for the FGN-NCZ coating. The formation of tribological iron oxide layer on FGN-NCZ coating is responsible for low mass loss of this coating.

The EDX maps of the FGN-NCZ wear track confirmed that the pin was worn during the test. The Fe element existed inside the track considerably higher than two unworn sides and also than other coatings as qualitatively shown in Fig. 11. Table 3 shows a quantitative measure for the iron oxide remained on the tribological layer. It appears that material removal takes place from steel pin during sliding. This material oxidizes on wear track and forms the iron oxide layer between contact pairs [28].

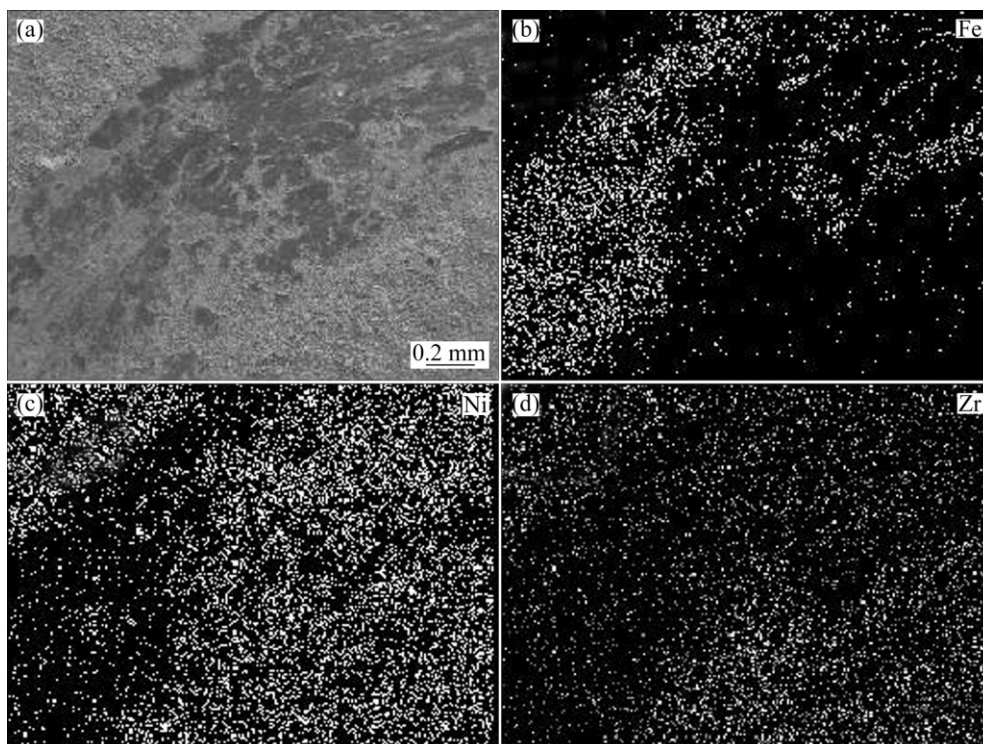


Fig. 11 SEM image (a) and EDX maps (b, c, d) of wear track on FGN-NCZ coating

Table 3 EDX analysis results of worn surface of FGN-NCZ coating

Sample	w(Ni)/%	w(Zr)/%	w(Fe)/%	w(O)/%
Without tribological layer	70.51	19.88	0.37	9.24
With tribological layer	47.14	12.33	22.63	17.89

3.2.3 Adhesion

Figure 12 shows the ON-NCZ and FGN-NCZ coatings after bending test. It can be seen that the density and the created crack width in the ON-NCZ coating are more than FGN-NCZ. This confirms that the FGN-NCZ

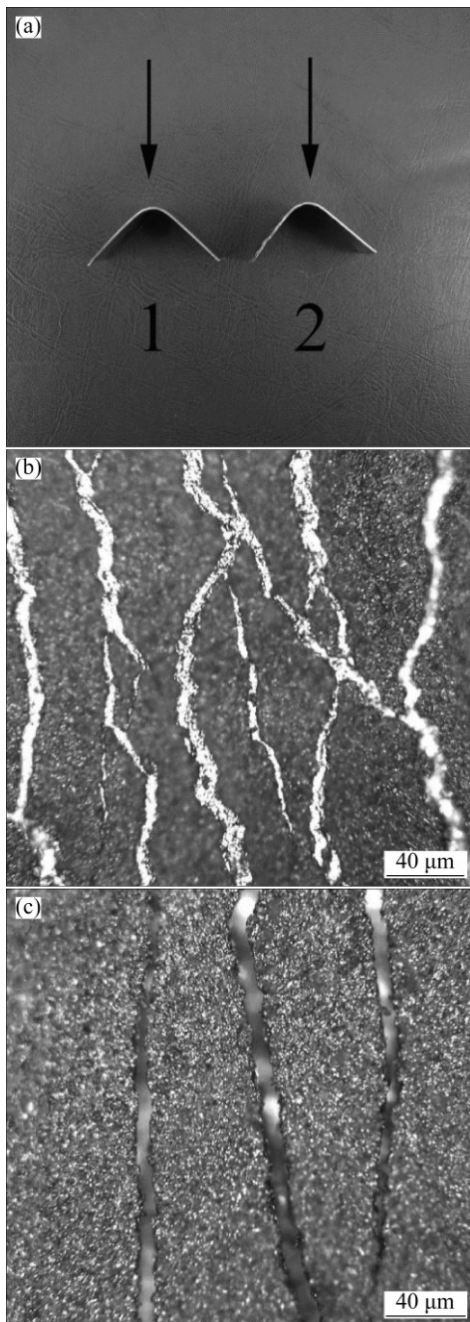


Fig. 12 Bending test results: (a) Typical samples after bending test; (b) Cracked ON-NCZ coating after test; (c) Cracked FGN-NCZ coating after test

coating possesses better adhesion ability and ductility compared with the ON-NCZ of the same outer surface hardness. Due to the fact that the coating microhardness decreased by moving from its surface to the interface as the result of coarser grain sizes, and the direct relationship between microhardness and elastic modulus, the elastic modulus of the FGN-NCZ coating approaches to that of the substrate. Therefore, the adverse effect of mechanical mismatch is diminished. The gradual increase in the microhardness by moving from the interface towards the surface of the coating accompanied with reduction in the internal stresses to the lowest magnitude is originated from the difference in the mechanical properties [18]. Hence, an advantage of the gradient composite coating deposit by electrodeposition is the possibility of decreasing the internal stress. Such a potential could confer the ability of fatigue-resistive property to the composite coatings used in industry especially in high tensile stress [30]. It could improve the mechanical properties and increase the life time of FGN-NCZ coated parts in the industry.

4 Conclusions

1) The use of electroless Ni plated ZrO_2 (NCZ) powders as second phase particles in the CED of Ni matrix composite coating results in the formation of Ni-NCZ (ON-NCZ) composite coating.

2) Stirring rate of the electroplating bath plays an important role in co-electrodeposition of second phase particles in composite coatings. For ON-NCZ, the maximum particle content of NCZ, best particle distribution and the maximum microhardness are achieved for electroplated sample in the bath at a stirring rate of 250 r/min. As well as, the functionally graded Ni-NCZ (FGN-NCZ) composite coating was successfully deposited by gradual increase of stirring rate from 0 to 250 r/min in the bath during electrodeposition.

3) Microhardness uniformly ascended from HV 580 near the substrate/coating interface and finally reached HV 730 on the surface for FGN-NCZ coating. Such a raise has been obtained due to simultaneous effects of the gradual increase in co-electrodeposited NCZ particles and the decrease in Ni matrix grain size from the interface towards the surface.

4) FGN-NCZ coating possesses better adhesion ability and ductility compared with the ON-NCZ coating of the same outer surface hardness which may be induced by decrease in mechanical mismatch between the coating and its substrate in the FGN-NCZ coating.

5) FGN-NCZ coating showed higher wear resistance than ON-NCZ coating. This was due to the formation of iron oxide layers and resistance to cracking

during wear process. The microstructure changes of FGN-NCZ were recognized as the reason of this behavior. These changes lead to decrease in stress concentration and proper adhesion between coating and substrate at the interface.

References

- [1] ARGHAVANIAN R, BOSTANI B, PARVINI AHMADI N. Characterisation of coelectrodeposited Ni–Al composite coating [J]. *Surface engineering*, 2015, 31: 189–193.
- [2] ARGHAVANIAN R, BOSTANI B, PARVINI AHMADI N, YAZDANI S. Field-enhanced co-electrodeposition of zirconia particles with a magnetic shell during Ni electrodeposition [J]. *Surface and Coating Technology*, 2014, 258: 1171–1175.
- [3] ADABI M, AMADEH A. Electrodeposition mechanism of Ni–Al composite coating [J]. *Transactions of Nonferrous Metals Society of China*, 2014, 24: 3189–3195.
- [4] BOSTANI B, ARGHAVANIAN R, PARVINI-AHMADI N. Study on particle distribution, microstructure and corrosion behavior of Ni–Al composite coatings [J]. *Materials and Corrosion*, 2012, 63: 323–327.
- [5] HAJIALI FINI M, AMADEH A. Improvement of wear and corrosion resistance of AZ91 magnesium alloy by applying Ni–SiC nanocomposite coating via pulse electrodeposition [J]. *Transactions of Nonferrous Metals Society of China*, 2013, 23: 2914–2922.
- [6] ADABI M, AMADEH A. Formation mechanisms of Ni–Al intermetallics during heat treatment of Ni coating on 6061 Al substrate [J]. *Transactions of Nonferrous Metals Society of China*, 2015, 25: 3959–3966.
- [7] ARGHAVANIAN R, PARVINI-AHMADI N. The effect of co-electrodeposited ZrO₂ particles on the microstructure and corrosion resistance of Ni coatings [J]. *Journal of Solid State Electrochemistry*, 2011, 15: 2199–2204.
- [8] BIN C, TAN Y F, LONG H, HUA T A, LI G A. Tribological properties of TiC particles reinforced Ni-based alloy composite coatings [J]. *Transactions of Nonferrous Metals Society of China*, 2013, 23: 1681–1688.
- [9] ARGHAVANIAN R, PARVINI-AHMADI N, YAZDANI S, BOSTANI B. Investigations on corrosion proceeding path and EIS of Ni–ZrO₂ composite coating [J]. *Surface Engineering*, 2012, 28: 508–512.
- [10] ARGHAVANIAN R, PARVINI-AHMADI N. Electrodeposition of Ni–ZrO₂ composite coatings and evaluation of particle distribution and corrosion resistance [J]. *Surface Engineering*, 2011, 27: 649–654.
- [11] LAMPKE T, DIETRICH D, LEOPOLD A, ALISCH G, WIELAGE B. Cavitation erosion of electroplated nickel composite coatings [J]. *Surface and Coatings Technology*, 2008, 202: 3967–3974.
- [12] NIU Z X, CAO F H, WEI W A, ZHANG Z, ZHANG J Q, CAO C N. Electrodeposition of Ni–SiC nanocomposite film [J]. *Transactions of Nonferrous Metals Society of China*, 2007, 17: 9–15.
- [13] ORLOVSKAJ L, PERIENE N, KURTINAITIENE M, BIKULCIUS G. Electocomposites with SiC content modulated in layers [J]. *Surface and Coating Technology*, 1998, 105: 8–12.
- [14] KIM S K, YOO H J. Formation of bilayer Ni–SiC composite coatings by electrodeposition [J]. *Surface and Coating Technology*, 1998, 108: 564–569.
- [15] JASIM K M, RAWLINGS R D, WEST D R F. Metal-ceramic functionally gradient material produced by laser processing [J]. *Journal of Material Science*, 1993, 28: 2820–2826.
- [16] DONG Y S, LINA P H, WANG H X. Electroplating preparation of Ni–Al₂O₃ graded composite coatings using a rotating cathode [J]. *Surface and Coating Technology*, 2006, 200: 3633–3636.
- [17] KOKINI K, CHOULES B D. Surface thermal fracture of functionally graded ceramic coatings: Effect of architecture and materials [J]. *Composite Engineering*, 1995, 5: 865–877.
- [18] WANG L P, GAO Y, XUE Q J, LIU H W, XU T. Graded composition and structure in nanocrystalline Ni–Co alloys for decreasing internal stress and improving tribological properties [J]. *Journal of Physics D: Applied Physics*, 2005, 38: 1318–1324.
- [19] LI J, DAI C, WANG D, HU X. Electroforming of nickel and partially stabilized zirconia (Ni + PSZ) gradient coating [J]. *Surface and Coating Technology*, 1997, 91: 131–135.
- [20] DING X M, MERK N. Improvement of wear and adherence properties of composite coatings by a gradual increase in particle volume fraction [J]. *Scripta Materialia*, 1997, 37: 685–690.
- [21] BANOVIC S W, BARMAK K, MARDER A R. Characterization of single and discretely stepped electro-composite coatings of nickel–alumina [J]. *Journal of Material Science*, 1999, 34: 3203–3211.
- [22] WANG H, YAO S, MATSUMURA S. Electrochemical preparation and characterization of Ni/SiC gradient deposit [J]. *Journal of Materials Processing Technology*, 2004, 145: 299–302.
- [23] ARGHAVANIAN R, PARVINI AHMADI N, YAZDANI S, BOSTANI B. Fabrication and characterisation of nickel coated Ni-NCZ (nickel coated ZrO₂) composite coating [J]. *Surface Engineering*, 2012, 28: 503–507.
- [24] LARI BAGHAL S M, HEYDARZADEH SOHI M, AMADEH A. A functionally gradient nano-Ni–Co/SiC composite coating on aluminum and its tribological properties [J]. *Surface and Coating Technology*, 2012, 206: 4032–4039.
- [25] LEE E C, CHOI J W. A study on the mechanism of formation of electrocodeposited Ni–diamond coatings [J]. *Surface and Coatings Technology*, 2001, 148: 234–240.
- [26] BOSTANI B, PARVINI AHMADI N, YAZDANI S. Manufacturing of functionally graded Ni–ZrO₂ composite coating controlled by stirring rate of the electroplating bath [J]. *Surface Engineering*, 2016, 32: 495–500.
- [27] TJONG S C, LAU K C. Tribological behavior of SiC particle-reinforced copper matrix composites [J]. *Materials Letters*, 2000, 43: 274–280.
- [28] HOU K H, GER M D, WANG L M, KE S T. The wear behaviour of electro-codeposited Ni–SiC composites [J]. *Wear*, 2002, 253: 994–1003.
- [29] CHOI I S, DAO M, SURESH S. Mechanics of indentation of plastically graded materials — I: Analysis [J]. *Journal of the Mechanics and Physics of Solids*, 2008, 56: 157–171.
- [30] HADIAN S E, GABE D R. Residual stresses in electrodeposits of nickel and nickel–iron alloys [J]. *Surface and Coating Technology*, 1999, 122: 118–135.

功能梯度镀镍 ZrO_2 复合涂层的共同电沉积和性能评价

B. BOSTANI¹, N. PARVINI AHMADI¹, S. YAZDANI¹, R. ARGHAVANIAN²

1. Faculty of Materials Engineering, Sahand University of Technology, Tabriz 53317-11111, Iran;

2. Department of Mechanical Engineering, Tabriz Branch, Islamic Azad University, Tabriz, Iran

摘要: 通过逐步提高搅拌速率, 成功从电镀槽中共同电沉积化学镀镍 ZrO_2 (NCZ)功能梯度 Ni-NCZ 复合涂层。研究表明, 在搅拌速度为 250 r/min 的电镀槽中, 共同电沉积导致最大颗粒含量和最佳颗粒分布。为制备 NCZ 梯度 Ni-NCZ 复合涂层, 搅拌速度从 0 不断增加至 250 r/min。从基体到表面共沉积的 NCZ 含量持续增加。结果表明, 随着镍基体中共同电沉积的 NCZ 粒子含量的增加, 从界面到涂层表面显微硬度增加。镍基体较小的晶粒尺寸和较高的共同电沉积颗粒含量是显微硬度提高的原因。弯曲试验表明, 与普通 Ni-NCZ 涂层相比, 功能梯度复合涂层与基体具有更好的附着力, 这一结果归因为功能梯度复合涂层与基体之间具有更好的机械匹配。耐磨测试结果表明, 功能梯度 Ni-NCZ 复合涂层的耐磨性优于普通复合涂层。

关键词: 共同电沉积; 功能梯度复合涂层; 显微硬度; 耐磨性; 附着力

(Edited by Xiang-qun LI)